Review on Material Synthesis and Characterization of Sodium (Na) Super-Ionic Conductor (NASICON)

Review on Material Synthesis and Characterization of Sodium (Na) Super-Ionic Conductor (NASICON)

M I Kimpa[1,2], M Z H Mayzan[1], J A Yabagi[1,3], M M Nmaya[1,3], K U Isah[2], M A Agam[1*]

[1]Department of Science, Faculty of Applied Sciences and Technology, Bandar University, 84600, Universiti Tun Hussein Onn Malaysia,84500, Pagoh, Johor, Malaysia.
[2]Department of Physics, School of Physical Sciences, Federal University of Technology Minna, P.M.B 65, Minna, Niger State, Nigeria.
[3]Department of Physics, Faculty of Science, Ibrahim Badamasi Babangida University Lapai, P.M.B. 10, Lapai, Niger State, Nigeria.

Corresponding email: arif@uthm.edu.my

Abstract. Sodium (Na) Super Ionic Conductor (NASICON) has general formula $Na_{1+x}Zr_2P_{3-x}Si_xO_{12}$ ($0 \leq x \leq 3$) derived from its parent compound, sodium zirconium phosphate $NaZr_2(PO_4)_3$ (NZP) which belong to a rhombohedral crystal structure. This material consists of three-dimensional structure with interesting features such as low thermal expansion coefficient, thermal stability, gas sensor and nuclear waste immobilization that make it viable for industrial applications. Current study presents comprehensive studies on the synthesis and essential characteristics required to understand the theory behind the mechanism that justifies the study of NASICON structure and its application such as lithium ion rechargeable battery, gas sensor, and nuclear waste immobilization and so on.

1. Introduction

The compounds $Na[Ge, Ti, Zr]_2(PO_4)_3$ have been studied since early 60s and the structure was named as sodium super ionic conductor (NASICON) in 1976 by Hong [1]. This decision was postulated after the discovery of β-alumina by Yao and Kummer [2]. β-Alumina ($Na_2O.11Al_2O_3$) has a layer structure and fast Na^+ ion conductor that migrate between two-dimensional Na^+ conductive planes situated between the Al_2O_3 spinel blocks [3]. Hong proposed a framework structure with suitable tunnel size for Na^+ migration in three dimensional plane [1], [4].

In the pioneering work of Hong [1], the possibility of synthesizing series of materials with general formula $Na_{1+x}Zr_2Si_xP_{3-x}O_{12}$ ($0 \leq x \leq 3$) has been demonstrated [5] and the study achieved an excellent ionic conductor for the material of $Na_3Zr_2Si_2P_3O_{12}$ at a stoichiometry ratio when $x = 2$ [6]. The conductivity of $Na_3Zr_2Si_2PO_{12}$ above 443 K was found to be comparable to that of Na-*b*- alumina ($Na_2O_xAl_2O_3$), with many advantages in practical applications as fast ion conductor [2]. Since then, various ionic conductors have been discovered and numerous applications have been found [7], [8].

The special attraction of the NASICON lies in its structure. Several interesting features such as low thermal expansion coefficient, thermal stability, gas sensor and nuclear waste immobilization make it viable for industrial applications. Superionic conductors are compounds that have high ionic conductivity at elevated or room temperatures. Based on the general formula of this nature $AMM'(PO_4)_3$,

where site "A" is the mobile ions which are generally Li^+, Na^+ or K^+ but higher valent elements have also been observed. M and M′ can be occupied by di-, tri-, tetra- or penta- cation [4,5]. The P site can be partially substituted by Si. Thus, the structure is very flexible for substitution at A, M, M′ and P sites giving rise to a large number compounds for a comparative study. All these compounds share the same topology in their framework irrespective of the presence of sodium or exhibition of high ionic conduction [11].

The NASICON crystal structure is described as illustrated in Figure 1 showing MO_6 octahedra linked with PO_4 tetrahedra to form 3D interconnected network with two interstitial sites where mobile cation (Li^+) are distributed [7,8]. In this structure, conductor cations in the interstitial sites move from one site to the next by jumping through bottlenecks between the two polyhedral. The size of the bottleneck depends on the nature of the skeleton ions and the carrier concentration in both type of the sites (M′ and M″) [9,10]. The rigid frame work $[M_2(PO_4)_3]^-$ which balances with electron from Li^+ ions is located only at M′ site along c-axis with a distorted octahedral coordination. Substitution of lower valance electron such as tri-cations atoms at P-site allows the percolation of electron to move towards M″ and conduction occur [16].

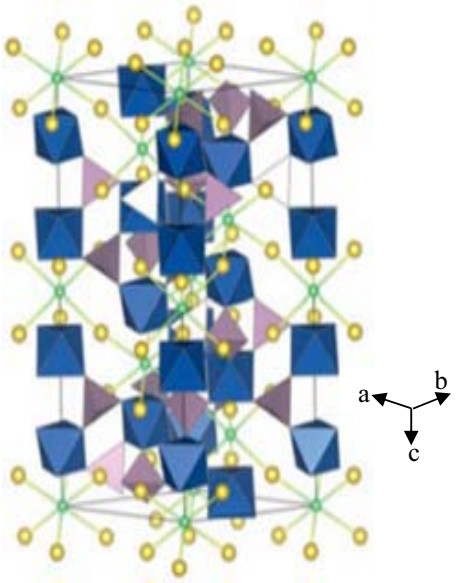

Figure 1: Schematic diagram of NASICON-type 3D structure of $LiM_2(PO_4)_3$ [17].

Most of Nasicon type systems can crystallize in hexagonal or rhombohedral lattices and few of them crystallize in monoclinic, langbeinite, garnet, SW type (orthorhombic scandium wolframate $Sc_2(WO_4)_3$) lattices [13–15]. This compound has unusual property of accommodating 40 to 45 elements in its structure and also have some special structural features such that all the atoms, except oxygen, can be substituted by various atoms of different oxidation states and radii, giving the resulting compositions different chemical and physical properties, while at the same time retaining the main crystal structure [21]. This make it amiable for diverse applications for block engines, electrical vehicles and mobile electronic devices [22].

2. Synthesis of NASICON Ceramic

There are several ways of synthesizing NASICON ceramics materials based on the application in view, stability and densification parameter required. Most of these materials are prepared in polycrystalline structure with various advantages.

2.1 Solid State Reaction Method

Solid state reaction method is one of the techniques that are widely used to prepare starting materials solid mixture, such as, polycrystalline solids. These materials do not react with each other at room temperature over a period of time but require high temperature to heat the materials to the suitable reaction rates. Chemical reaction involved in this technique comprises of a large number of compound which are feasibly to increase the rate of solid reaction through their structural properties of the reactants and surface area of the mixed precursor. Thermodynamics free energy change that is associated with the rate of chemical reaction is one of the factors that contribute to the solid state reaction process. Generally, two-thirds of the melting temperature of one component is enough to activate diffusion sufficiently, to enable solid state reaction. The advantages of solid state reaction over other preparation techniques were availability of the starting precursor for the synthesis and production of more final product in large quantity as well as low cost of production to meet the industrial scale demands. Solid state reaction method also has some disadvantages due to high temperature synthesis such as undesirable phases that do precipitate sometimes but it is outweighed by its numerous advantages [21].

2.2 Sol-Gel Method

Sol-gel technique consists of converting the sol; a concentrated or colloidal suspension of the reactants which is then concentrated or matured to form the 'gel', the homogenous gel is then heat-treated to form the product. This method is frequently employed to synthesize various materials due to their several advantages, which include good mixture of the reagents, relatively low crystallization temperature and small grain size of the product [23], [24].

These advantages could be viewed in comparison with the raw materials high cost, the long processing time involved, the non-uniformity of the films, and the formation of cracks upon drying. This technique could not be adopted in this research because it is very difficult to control the reaction rate process, its pH value and amount of complexing agent during material preparation. During high homogeneous precursor, it is difficult to avoid the precipitation of PO_4^{3-} for the composition contained the partial substitution of Ti^{4+} and Al^{3+} [25].

2.3 Spark Plasma Sintering Method

Spark plasma sintering (SPS) is a fast-sintering technique used to prepare dense ceramics [26]. In principle, during SPS processing, a DC current and pressure are uploaded on the sample and the current run through the graphite die that is taken as the external heat source. Such a heating method enables samples to be compacted within a very short time at low temperature, and obvious grain growth can be suppressed. The enhanced densification by SPS has been observed in several metallic, ceramic, and multi-layer systems, especially in difficult-to-sinter materials such as $SiC–Al_2O_3$, PMM-Pt and LTP [27]. In addition, a relatively low sintering temperature with a minimal grain growth in SPS has been applied to fabricate nanostructures materials. It has indicated that the ionic conductivity of solid electrolytes can be improved substantially by decreasing the grain size to nanoscale. SPS techniques was used to study ionic conductivity of LTAP composition and found the conductivity increases to 1.12×10^{-3} Scm^{-1} [28].

2.4 Microwave Method

A more effective method of synthesis has been proposed using microwave heating which results in products exhibiting high phase purity, good crystalline and minimal loss of volatile constituents. Microwave processing techniques is a technology that process new material, powerful and important tools that can process materials that may not be amendable to conventional means of processing materials or to improve the performance characteristics of the existing materials [29].

Microwaves are not forms of heat but rather forms of energy that are manifested as heat through their interaction with materials. Microwaves initially excite the outer layers of molecules. The inner part of the material is warmed as heat travels from the outer layers inwards. Most of the moisture is vaporized

before leaving the material. If the material is very wet and the pressure inside rises rapidly, the liquid will be removed from the material due to the difference in pressure. This creates a sort of pumping action forcing liquid to the surface, often as vapor [30]. This results into a very rapid drying, without the need to overheat the atmosphere and perhaps, it can cause case hardening or other surface overheating phenomena. It has been used to prepare NZP compositions, Alumina, Ziconia, ZnO, among others [31]. It is low cost, has high heating rates, low sintering time, uniform and volumetric heating, low temperatures and improved mechanical properties, dense materials among others [24,26,27].

2.5 Ion Exchange

Solid electrolytes are ideal materials for carrying out ion exchange reactions since they have mobile ions of one type within a rigid host framework [33]. With ion exchange methods, new materials can be synthesized between the ion exchange and the solution. The chemical analysis in most cases is not complete and yield formation of different structure [34]. Some of these new materials may have properties or structures that are of technological importance. Moreno-Real used ion exchange to prepare NASICON glass ceramic in a compound containing mixed ion and has low ionic mobility. Sodium cations remain within v-$Li_3Al_2(PO_4)_3$, which could be one of the main reasons for the low mobility of both alkaline cations, suggesting the presence of a mixed cation effect [19]. Gaubicher *et al*. studied B-$Li_3V_3(PO_4)_3$ NASICON material using ion exchange techniques under constant gas flow of 10% H_2 in N_2 for 3 x 20 h at 900 °C. The exchange of Na^+ with Li^+ was affected due to stirring of the B-NVP powder in concentrated aqueous solution. This techniques is not frequently studied because is very difficult to know the rate at which the chemical reaction is complete [35].

2.6 Hydrothermal Method

Hydrothermal is a synthesis method of growing a single crystal from an aqueous solution at a high temperature range. Hydrothermal synthesis is considered as a high temperature technique, even though the temperatures are low compared to most traditional melt techniques. It has the advantage of rapid growth rates because of the rapid diffusion processes and it is a method of growth technique from liquid solution with lower viscosity of liquid [36]. The advantage of this technique is that reactions do not require much time compared to conventional methods and most compounds with unusual oxidation state element can be synthesized [37]. It involves heating the reactants in a closed vessel, for example, the autoclave with water.

2.7 Melt Quenching Method

Melt quenching technique is the most popular method used to prepare glasses [33,34]. The glass is prepared by heating the precursors at a temperature above its melting point, and rapidly cooled. Thus, mercury, water or liquid nitrogen is assisted for the quenching or cooling processes. Faster quenching process gives a more amorphous result. It slows the crystallization process due to the shorter time required for the atom to arrange its crystal lattice. However, samples produced from this method cannot be fabricated into desired shape and are hard to fabricate. Moreover, an extra precaution has to be taken especially when handling the chemicals used in the quenching processes.

3. Characterization Techniques

3.1 X-Ray Diffraction Techniques

X-ray diffraction (XRD) is one of the primary techniques that can be used to determine the crystalline structure, its orientation and lattice parameters of solid materials. When X-rays interact with atoms in the crystal lattices of a solid, a diffraction pattern is generated. Since each crystalline solid has a unique atomic orientation, the generated XRD pattern is characteristic of the material from which is obtained and can be used as a fingerprint to identify the crystalline phases and its structure.

An English physicist Sir W.H. Bragg and his son Sir W.L. Bragg developed a relationship in 1913 to explain why the incident X-ray beams reflects at certain angles when they interact with atoms of crystalline phases of the solids. When X-rays interact with atoms in two lattice planes, and the path length difference between rays equals a whole multiple of the wavelength of the radiation, constructive interference occurs, which is illustrated in (Figure 2). Bragg's law (Eq. 1) describes the conditions for constructive interference in certain directions and the production of diffracted scattered X-rays where n is an integer, λ is wavelength, d is spacing between atomic planes and θ is the angle of incidence. More so, Bragg's law reveals the crystallographic details of the samples.

$$n\lambda = 2d \sin\theta \tag{1}$$

X-rays are electromagnetic waves or photons with energy $E = hc/\lambda$, where h is the plank's constant ($6.62607004 \times 10^{-34}$ m^2 kg / s), c is the speed of light (3 x 10^8 m/s) and λ is the wavelength in Ångström (10^{-10} m). The atom sizes and the distances between the atoms (d-spacing) provide an explanation of the x-ray scattering of crystalline materials that is useful for crystal structure determination. X-rays are scattered by atoms in the different crystalline planes (hkl) and are picked up by the detector, which then converts them into intensity against 2θ spectrum. The XRD analysis enables us identify the material without destroying the sample.

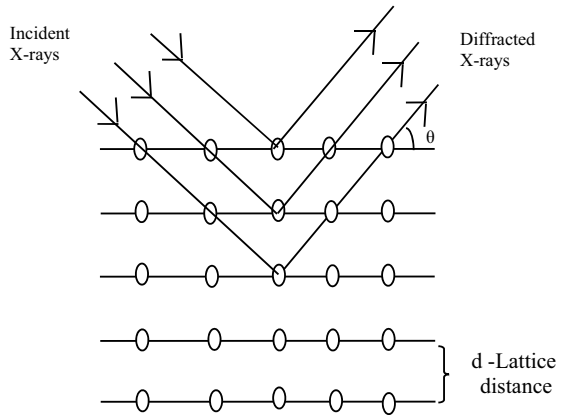

Figure 2: Schematic diagram showing the basic principles of X-ray diffraction

3.2 Theory of Crystal Structures

Crystalline materials are materials that atoms are situated in a repeating or periodic array over large atomic distances. These atoms upon solidification bonded together to their nearest neighbour in a repetitive three-dimensional pattern. All metals, ceramic materials and certain polymers form crystalline structures under normal solidification conditions while some materials do not crystallize and because they are non-crystalline or amorphous in nature. The properties of crystalline solids depend on the crystal structure of the material which describes the manner in which each atoms or ions or molecules are spatially arranged. There is an extremely large number of different crystal structures all having long range atomic order; these vary from simple structures for metals to complex ones, as displayed by some of the ceramic and polymeric materials.

Crystalline materials are composed of one or more crystalline phases. Each phase takes on one of the seven possible crystal lattice structures shown in Figure 3, which describe the symmetry of the crystal. The seven lattice systems can be divided into 14 categories called Bravais lattices, which can be further divided into 230 different space groups depending on the placement of atoms in the lattice.

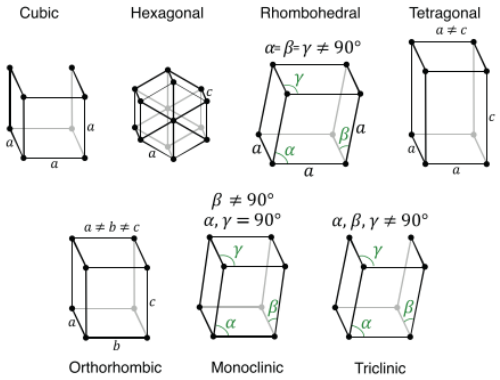

Figure 3: Seven 3-dimensional crystal lattice system

3.3 Fourier Transform Infrared Spectroscopy

Fourier transform infrared spectroscopy (FTIR) is a very powerful techniques used for identification of functional groups and an infrared spectrum of absorption, transmission, emission or photoconductivity of a material. Organic molecules absorb IR radiation between 4000 cm^{-1} and 400 cm^{-1} which correspond to absorption energy of 11 kcal/mole and 1 kcal/mole. This is the amount of energy that initiates the transition between the vibrational states of bonds that is contained within the molecules. The most important regions of the IR spectrum are the regions > 1650 cm^{-1} and the finger print region (600 – 1500 cm^{-1}). The finger print regions cannot easily be used for identification of unknown compounds. Thus, many references exist to identify the IR frequencies for various functional groups and organic compounds [40].

Light is composed of electric and magnetic waves known as electric vector and magnetic vectors which can be described as electromagnetic radiation. Since the motion of wave is repetitive, they go through cycles. These cycles begin at zero amplitude and ends when the wave has crossed zero amplitude for the third cycle. The travel distance by a wave during a cycle is called wavelength (distance per cycle) but only distance as unit of wavelength is noted.

Another important property of a light wave is its wavenumber which measures the number of cycles a wave undergoes per unit length. Wavenumber are measured in units of cycles per centimetre, which are often represented as cm^{-1}. Most infrared spectra are plotted from 4000 to 400 cm^{-1} along the x-axis. The two quantities (wavelength and wavenumber) are related as reciprocals of each other in eq. 2 where ω = wavenumber and λ = wavelength. Since the wavelength is measured in centimetres, wavenumber is calculated in cm^{-1}.

$$\omega = 1/\lambda \tag{2}$$

Thus, wavenumber is proportional to the energy of a light wave and they are related as in eq. 3 where E = Light energy in Joules, c = the velocity of light (~3 X 10^{10} cm/second), h = Planck's constant (6.63 X 10^{-34} Joule-second), ω = wavenumber. The different properties of light waves are related to each other by the relation in eq.4 where c, λ and υ have their usual meaning.

$$E = hc\,\omega \tag{3}$$

$$c = \nu\lambda \tag{4}$$

In Conventional IR spectrophotometer, a sample IR beam is directed through the sample chamber and measured against a reference beam at each wavelength of the spectrum. The entire spectral region must be scanned slowly to produce good quality spectrum. This mechanism is built-up with the principle of Michelson Interferometer (Figure 4). The radiation from IR source is directed through the sample cell and was split 50:50 through the beam splitter. One of the radiations is reflected from a fixed mirror while the other half is reflected from the mirror which introduced different optical path lengths. These beams were reflected by the mirrors and recombined to create an interference signal called an interferogram. The interferogram is a unique signal resulting from the constructive and destructive interferences (due to different optical paths) and contains all infrared frequencies.

The interferogram passed through the sample and the resultant interferogram is detected using the pyroelectric detector. Each molecular bond will couple with a specific frequency of light causing molecular bond vibrations and a signal in the interferogram. According to quantum mechanics, the molecular bonds vibrate by absorbing energy and excite from the lowest state to the highest (usually from the ground state to the first exited state). For a transition to be FTIR active, the molecule must undergo a dipole moment change during vibration. The resultant interferogram was finally Fourier transformed to generate intensity as a function of wavenumber.

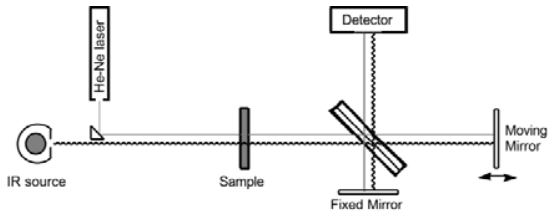

Figure 4: Diagram of the Michelson Interferometer used in FTIR spectrophotometer

3.4 Scanning Electron Microscopy/Elemental Dispersive X-Ray Techniques

In 1935, a German scientist known as Stylizing and Knoll invented the first Scanning Electron Microscopy (SEM). Zworykin from USA in 1942 later developed the first version of SEM, but there were some challenges relating to signal to noise ratio of SEM images. Nixon and Oatly in 1950, further designed SEM with modern technology in Cambridge University. Research was ongoing on how to commercialize the production of SEM when Stewart and Snelling built the first commercial SEM in 1965. The computer program has been attached to the recent SEM in order to increase its analysis ability and to solve some other problems found in the previous versions like signal-to-noise ratio [41].

Scanning electron microscopy (SEM) is a type of electron microscope that uses a focused beam of high energy electrons to produce images of a sample by creating various signals at the surface of the sample. These signals are generated by the electron-sample interaction and provide information about the sample; for instance, sample external morphology, crystalline structure and chemical composition [42]. SEM works by creating an electron beam with high energy produced by an electron gun. The electron beam will be controlled by a series of lenses and apertures. When the electron beam arrives to the surface of the specimen, electron-sample interaction will occur and several types of signals will be generated. Different types of detectors to produce SEM images can detect these signals. SEM machine operates at a high vacuum level to avoid the contamination [41]. A typical SEM layout is shown in (Figure 5).

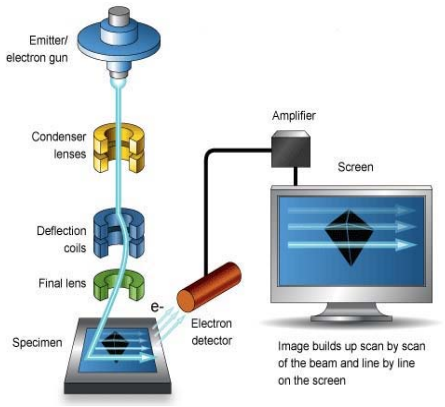

Figure 5: SEM layout showing the major component

There are some limitations for SEM to be used for image analysis, SEM samples must be solid and dry powder. Living cells, soft bodies and tissues cannot be used directly unless it undergoes some sample preparation. In addition, all samples must be stable under the high vacuum system of SEM because the vacuum system can destroy some unstable samples. We have different electron sources in SEM; one is the secondary electron source. This source is more affected for morphological investigations of organic and inorganic specimens. Secondary electrons provide great information about the structure of the specimen with a resolution down to the nanometre range. While the backscattered electron source gives compositional images for the samples to know the chemical components and bonding differences within the specimen. Chemical compositions of a specimen could be detected by characteristics x-rays as one of the electron source in SEM techniques.

SEM is coupled with elemental dispersive x-ray (EDS) detector which identifies the element composed in the specimen. When primary electron beam hits the samples, some electrons will be removed from some orbits in the sample and these electrons will form X-rays. Obtaining X-rays will be helpful to get elemental information about the specimen. The EDS used as X-rays detectors. EDS detects the element of the sample contrary to the principle that each element has a unique atomic structure and energy difference between different discrete electron states. When one electron in the lower energy state is ejected to an excited state or out of the shell, there is a hole left which is then filled by an electron at the higher energy state, during this process an x-ray is emitted and detected by corresponding detector, forming a set of peaks characteristic of each element. Thus, EDS cannot detect elements with an atomic number less than 5.

3.5 Impedance Spectroscopy study of NASICON

Impedance spectroscopy (IS) is a powerful technique involving small alternative current (AC) signals for studying the conductivity of ionic conductors in solid or liquid, mixed conductors having electronic and ionic conductivity and effect of electrode-electrolyte interface. IS can also be used for studying dielectric behaviour of materials. Generally, impedance analysis of ionic solid materials identifies the elementary process such as the bulk conduction, ionic transport, grain boundary conduction and the electrode-electrolyte interface in a measured frequency domain.

In principle, the approach for the measurement of IS consist of the electrical current, $i(t)$ at certain angular frequency (ω), when a certain ac voltage, $v(t)$ is applied to the system (Figure 6). The impedance $Z(t)$ is given by:

$$Z(t) = \frac{v(t)}{i(t)} \tag{5}$$

The applied voltage *v* is defined as:

$$v(t) = v_o \sin(\omega t) \tag{6}$$

And the resulting electric current *i* is given by:

$$i(t) = i_o \sin(\omega t + \theta) \tag{7}$$

where θ is the phase difference between $i(t)$ and $v(t)$, v_o is the maximum voltage, i_o is the maximum current and $\omega = 2\pi f$ angular frequency.

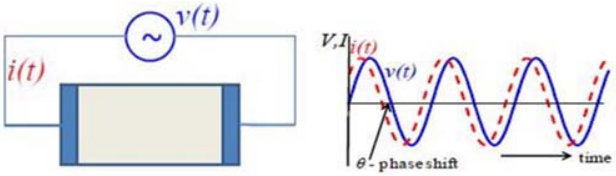

Figure 6: Schematic diagram of Impedance Spectroscopy operational principle

3.5.1 Complex Impedance and Equivalent Circuit analysis

Complex impedance analysis for a real system (i.e. solid electrolyte) has been shown in Fig. 7 (a). In this illustration, the impedance spectrum shows an inclined straight line which is due to the presence of double layer capacitance of electrode-electrolyte interface, a depressed semicircle is due to the macroscopic properties of the distributed materials and is termed as the bulk contribution to ionic conductivity. The high frequency region of the impedance plot along x-axis represents the ohmic resistance of the cell which is mainly related to the electrolyte material. The circuit is comprised of a series resistance (R_s) a charge-transfer resistance, (R_{ct}), a constant phase element (CPE1) and a spike CPE2. This curve can be fitted using an equivalent circuit given in Fig. 7 (b) where R_s indicate the ohmic resistance of the cell, *Rct* is the electron transfer resistance at the active interface (grain boundary for solid electrolyte ceramics). CPE reflects the interfacial capacitance. CPE2 is described as electrode-electrolyte interface caused by a finite diffusion of Li^+ ion in the electrolyte.

The theory of equivalent circuit analysis for impedance measurement is that, it provides information on the resistance, R and CPE, which lead to quantitative measurement of the conductivity, relaxation times and interfacial capacitance. The impedance spectrum of a polycrystalline materials mostly result into two semicircles due to the presence of grain boundaries. The grain boundary may act as a hindrance to ionic transport, but the presence of large defect density in the interfacial region could also contribute to the high conduction path. In this case, the bulk resistance of the sample is obtained from the high frequency region where the semicircles intersect with the real axis.

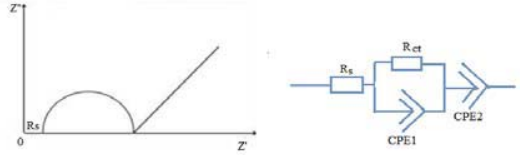

Figure 7: Impedance graph showing the Nyquist plot and its equivalent circuit.

3.5.2 Grain and Grain boundary concept

Grain boundary (GB) is the interface between two grains (G) or crystallites, in a polycrystalline material. Grain boundaries are defects in the crystal structure, and tend to decrease the electrical and thermal conductivity of the material. Generally, grain boundary is a planar defect that separates regions of different crystalline orientation (such as grains) within a polycrystalline solid. Grain boundaries are usually the result of uneven growth when the solid is crystallizing. Grain sizes vary from 1 μm to 1 mm. Most grain boundaries are preferred sites for the onset of corrosion and for the precipitation of new phases from the solid. They are also important to many of the mechanisms of creep. On the other hand, grain boundaries disrupt the motion of dislocations through a material and reduce crystallite size; this is a common way to improve the strength of a material. GB is a transition region where some atoms are not exactly aligned with either grain. Characterization of grain boundaries is of critical importance in materials studies. The properties of grain boundary determine the grain formation. Figure 8 illustrates the schematic example of grain and grain boundary.

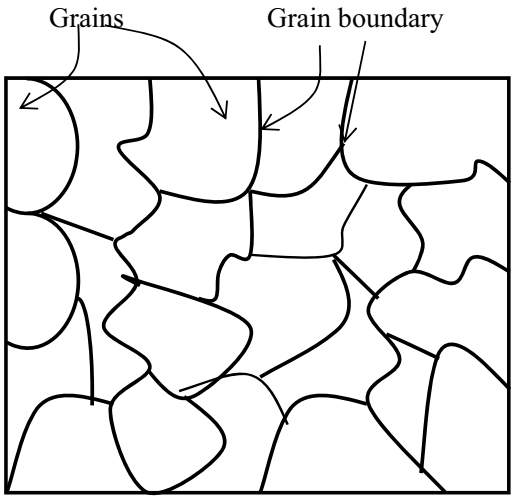

Figure 8: Schematic illustration of grain and grain boundary of a solid material

The study of grain boundary in this study is very important, due to great influence in increasing the ionic conductivity of solid electrolytes. Formation of secondary phases eliminate or reduced the grain boundary and achieved a good microstructure of glass ceramics in Nasicon material [43]. High conductivity of NASICON material due to formation of secondary phases ($AlPO_4$ and Li_2O) at grain boundary increase the ionic conductivity of LGAP [25].

3.5.3 Dielectric Properties

The dielectric constant (permittivity) describes the material behaviour in the electric field and consists of a real part, ε', called the dielectric constant, and an imaginary part, ε", called the dielectric loss factor. Thus, the permittivity is expressed as:

$$\varepsilon^* = \varepsilon' - j\varepsilon'' \tag{8}$$

where the dielectric constant indicates the ability of a material to store electric energy while the dielectric loss explains the loss of electric field energy in the material.

At microwave frequencies, ionic and electronic polarization mechanisms contribute predominantly to the net dipole moments and the permittivity. Figure 9 shows the variation of frequency with dielectric permittivity which basically have four basic mechanisms contributing to polarization [44];

i. Electronic polarization
ii. Ionic/atomic polarization
iii. Molecular/dipole/orientation polarization
iv. Space charge polarization.

A low dissipation factor (DF) is also required for low electrical losses in dielectric materials particularly at high frequency. Dissipation factor or loss tangent (tan δ) is the ratio of the dielectric constant's imaginary part to the real part, given by:

$$\tan\delta = \frac{\varepsilon''_r}{\varepsilon'_r} \tag{9}$$

A medium is said to be a good (lossless or perfect) dielectric if tan δ is very small ($\sigma << \omega\varepsilon'$) or a good conductor if tan δ is very large ($\sigma >> \omega\varepsilon'$). The characteristic behaviour of a medium also depends on the operational frequency ($f = \omega/2\pi$). A medium that is regarded as a good conductor at low frequency may be a good dielectric at high frequencies. The simplest way to define dissipation factor (loss tangent) is the ratio of the energy dissipated to the energy stored in the dielectric material. The more energy that is dissipated into the material the less is going to make it to the final destination. This dissipated energy typically turns into heat or is radiated as RF (radio frequencies) into the air. The optimal goal is to have 100 % of the signal pass through the interconnection network, and not be absorbed in the dielectric. With "high power" signals, a material with a large dissipation factor could result in the development of a tremendous amount of heat, possibly culminating in a fire (advanced dielectric heating). When the signals are very weak, a high-loss material means that little or no signal is left at the end of the transmission path. In order to retain maximum signal power, a low loss material should be used [44].

The dielectric loss tangent of materials represents quantitatively dissipation of the electrical energy to the various physical processes such as electrical conduction, dielectric relaxation and loss from linear processes. The total dielectric loss is the sum of intrinsic and extrinsic loss. Intrinsic dielectric loss depends on the crystal structure and can be described by the interaction of the phonon system with the AC electric field. The ac electric field alters the equilibrium of the phonon system and the subsequent relaxation associated with energy dissipation. The extrinsic losses are associated with the imperfections in the crystal lattice such as impurities, microstructural defects, grain boundary, porosity, micro crack, random crystallite orientation, dislocations, vacancies, dopant etc. The extrinsic losses are caused by lattice defects and therefore can in principle eliminated or reduce to the minimum by proper material processing.

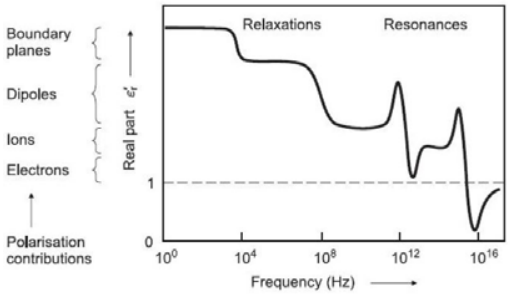

Figure 9 Polarization Mechanism [44]

4. Conclusion

The theoretical explanation and processes involved in synthesis and characterization techniques including the fundamental theories of impedance spectroscopy and dielectric properties have been highlighted for NASICON study. This could elaborate the scope of future researchers in areas of analyzing data based on the relevant theories discussed in this review. The application of NASICON ceramic materials in a large quantity for industrial production also depends on the fabrication method due to cheapness and environmental friendly.

Acknowledgement

The authors are grateful to the Federal University of Technology Minna and University Tun Hussein Onn Malaysia (UTHM) for their support and funding; this work is funded under incentive for publication grant (IGSP), U412 and graduate research incentive grant (GIPS), U301, UTHM.

References

[1] H. Y. Hong, "Crystal Structures and Crystal Chemistry in the system $Na_{1+x}Zr_2Si_xP_{3-x}O_{12}$," *Mat Res Bull*, vol. 11, pp. 173–182, 1976.

[2] Y.-F. Y. Yao and J. T. Kummer, "Ion Exchange Properties of and Rates of Ionic Diffusion in Beta-Alumina," *Journal of Inorganic and Nuclear Chemistry*, vol. 29, no. 1936, pp. 2453–2475, 1967.

[3] X. Lu, G. Xia, J. P. Lemmon, and Z. Yang, "Advanced materials for sodium-beta alumina batteries: Status, challenges and perspectives," *Journal of Power Sources*, vol. 195, no. 9, pp. 2431–2442, 2010.

[4] N. Anantharamulu, K. Koteswara Rao, G. Rambabu, B. Vijaya Kumar, V. Radha, and M. Vithal, "A wide-ranging review on Nasicon type materials," *Journal of Materials Science*, vol. 46, no. 9, pp. 2821–2837, 2011.

[5] W. Bogusz, F. Krok, and W. Piszczatowski, "Particular features of admittance spectra of polycrystalline NASICON samples," *Solid State Ionics*, vol. 119, no. 1, pp. 165–171, 1999.

[6] C. R. Mariappan, C. Galven, M. P. Crosnier-Lopez, F. Le Berre, and O. Bohnke, "Synthesis of nanostructured $LiTi_2(PO_4)_3$ powder by a Pechini-type polymerizable complex method," *Journal of Solid State Chemistry*, vol. 179, no. 2, pp. 450–456, 2006.

[7] Y. Liu, J. Chen, and J. Gao, "Preparation and chemical compatibility of lithium aluminum germanium phosphate solid electrolyte," *Solid State Ionics*, no. July, 2017.

[8] X. Lu, S. Wang, R. Xiao, S. Shi, H. Li, and L. Chen, "First-principles insight into the structural fundamental of super ionic conducting in NASICON $MTi_2(PO_4)_3$ (M = Li, Na) materials for rechargeable batteries," *Nano Energy*, vol. 2, 2017.

[9] P. Maldonado-Manso, M. C. Martín-Sedeño, S. Bruque, J. Sanz, and E. R. Losilla, "Unexpected cationic distribution in tetrahedral/octahedral sites in nominal Li1+xAlxGe2-x(PO4)3 NASICON series," *Solid State Ionics*, vol. 178, no. 1–2, pp. 43–52, 2007.

[10] Y. O. Korepina, L. S. Bigeeva, A. B. Il'in, A. I. Svitan'ko, S. A. Novikova, and A. B. Yaroslavtsev, "Cation mobility in Li1+xHf2−xScx(PO4)3 NASICON-type phosphates," *Inorganic Materials*, vol. 49, no. 3, pp. 287–292, 2013.

[11] A. Navulla, "Semi sol–gel synthesis, conductivity and luminescence studies of $Ca_{0.5}Fe_{1-x}Eu_xSb(PO_4)_3$ (x=0.1, 0.15 and 0.2)," *Solid State Ionics*, vol. 181, no. 13–14, pp. 659–663, 2010.

[12] K. He, C. Zu, Y. Wang, B. Han, X. Yin, H. Zhao, Y. Liu, and J. Chen, "Stability of lithium ion conductor NASICON structure glass ceramic in acid and alkaline aqueous solution," *Solid State Ionics*, vol. 254, pp. 78–81, 2014.

[13] C. Cao, Z.-B. Li, X.-L. Wang, X. Zhao, and W. Han, "Recent advances in inorganic solid electrolytes for lithium batteries," *frontiers in Energy Storage*, vol. 2, no. June, pp. 1–10, 2014.

[14] K. Arbi, M. Ayadi-Trabelsi, and J. Sanz, "Li mobility in triclinic and rhombohedral phases of the Nasicon-type compound $LiZr_2(PO_4)_3$ as deduced from NMR spectroscopy," *Journal of Materials Chemistry*, vol. 12, no. Icmm, pp. 2985–2990, 2002.

[15] N. V. Kosova, E. T. Devyatkina, A. P. Stepanov, and A. L. Buzlukov, "Lithium conductivity and lithium diffusion in NASICON-type $Li_{1+x}Ti_{2-x}Al_x(PO_4)_3$ (0<=x<= 0.3) prepared by mechanical activation," *Ionics*, vol. 14, no. 4, pp. 303–311, 2008.

[16] Y. Ren, K. Chen, R. Chen, T. Liu, Y. Zhang, and C. W. Nan, "Oxide Electrolytes for Lithium Batteries," *Journal of the American Ceramic Society*, vol. 98, no. 12, pp. 3603–3623, 2015.

[17] H. Eckert and A. C. Martins Rodrigues, "Ion-conducting glass-ceramics for energy-storage applications," *MRS Bulletin*, vol. 2, no. 3, pp. 206–212, 2017.

[18] E. Yi, W. Wang, S. Mohanty, J. Kieffer, R. Tamaki, and R. M. Laine, "Materials that can replace liquid electrolytes in Li batteries: Superionic conductivities in $Li_{1.7}Al_{0.3}Ti_{1.7}Si_{0.4}P_{2.6}O_{12}$. Processing combustion synthesized nanopowders to free standing thin," *Journal of Power Sources*, vol. 269, pp. 577–588, 2014.

[19] L. Moreno-Real, P. Maldonado-Manso, L. Leon-Reina, E. R. Losilla, F. E. Mouahid, M. Zahir, and J. Sanz, "Glasses and crystalline A3Al2(PO4)3 (A = Na, Li): an impedance and 31P, 27Al, 23Na and 7Li MAS-NMR study," *Journal of Materials Chemistry*, vol. 12, no. 12, pp. 3681–3687, 2002.

[20] H. Aono, "Studies on Li^+ Ionic Conducting Solid Electrolyte Composed of Nasicon-Type Structures," Osaka University, 1994.

[21] U. Ahmadu, A. O. Musa, N. Rabiu, and N. Nuntanwong, "Structural Characterization of Lithium Doped NZP $Na_{1-x}Li_xZr(PO_4)_3$ (x=0.00-0.75)," *Bayero Journal of Pure and Applied Sciences*, vol. 4, no. 1, pp. 135–144, 2011.

[22] J. Yang, Z. Huang, B. Huang, J. Zhou, and X. Xu, "Influence of phosphorus sources on lithium ion conducting performance," *Solid State Ionics*, vol. 270, pp. 61–65, 2015.

[23] Z. Xiao, S. Chen, and M. Guo, "Influence of Li_3PO_4 addition on properties of lithium ion-conductive electrolyte $Li_{1.3}Al_{0.3}Ti_{1.7}(PO_4)_3$," *Transactions of Nonferrous Metals Society of China*, vol. 21, no. 11, pp. 2454–2458, 2011.

[24] S. Breuer, D. Prutsch, Q. Ma, V. Epp, F. Preishuber-Pflügl, F. Tietz, and M. Wilkening, "Separating bulk from grain boundary Li ion conductivity in the sol–gel prepared solid electrolyte $Li_{1.5}Al_{0.5}Ti_{1.5}(PO_4)_3$," *J Mater Chem A*, vol. 3, no. 42, pp. 21343–21350, 2015.

[25] Z. Lin-chao, P. Chen, Z. Hu, and C. Chen, "Electrical Properties of NASICON-type Structured $Li_{1.3}Al_{0.3}Ti_{1.7}(PO_4)_3$ Solid Electrolyte Prepared by 1,2-Propylene glycol-assisted Sol-gel Method," *Chinese Journal of Chemical Physics*, vol. 25, no. 6, pp. 703–707, 2012.

[26] A. Mei, Q. H. Jiang, Y. H. Lin, and C. W. Nan, "Lithium lanthanum titanium oxide solid-state electrolyte by spark plasma sintering," *Journal of Alloys and Compounds*, vol. 486, no. 1–2, pp. 871–875, 2009.

[27] L. Ji-Sun, C.-M. Chang, Y. Il Lee, J.-H. Lee, and S.-H. Hong, "Spark Plasma Sintering (SPS) of NASICON Ceramics," *Journal of the American Ceramic Society*, vol. 87, no. 2, pp. 305–307, 2004.

[28] X. Xu, Z. Wen, X. Yang, and L. Chen, "Dense nanostructured solid electrolyte with high Li-ion conductivity by spark plasma sintering technique," *Materials Research Bulletin*, vol. 43, no. 8–9, pp. 2334–2341, 2008.

[29] S. Wang, L. Ben, H. Li, and L. Chen, "Identifying Li^+ ion transport properties of aluminum doped lithium titanium phosphate solid electrolyte at wide temperature range," *Solid State Ionics*, vol. 268, pp. 110–116, 2014.

[30] I. Ivan and W. Peter, "Microwave heating: Practical example," 2013.

[31] a. H. Naik, S. B. Deb, a. B. Chalke, M. K. Saxena, K. L. Ramakumar, V. Venugopal, and S. R. Dharwadkar, "Microwave-assisted low temperature synthesis of sodium zirconium phosphate (NZP) and the leachability of some selected fission products incorporated in its structure — A case study of leachability of cesium," *Journal of Chemical Sciences*, vol. 122, no. 1, pp. 71–82,

2010.
[32] U. Ahmadu, T. Salkus, A. O. Musa, and K. U. Isah, "Electrical and Dielectric Characterization of $Na_{0.5}Li_{0.5}Zr_2(PO_4)_3$," *Open Journal of Physical Chemistry*, vol. 1, pp. 94–103, 2011.
[33] U. Ahmadu, "NASICON: Synthesis, Structure and Electrical Characterization," in *Advanced Sensor and Detection Materials*, M. M. D. Ashutosh Tiwari, Ed. Scrivener Publishing LLC, 2014, pp. 265–308.
[34] Y. S. Savaskan, O. Hulisi, and H. Baki, "Synthesis of the New Cation Exchange Resins Having Poly (Styrene-Caprolactone) Units," *Tr J of Chemistry*, vol. 21, pp. 270–276, 1997.
[35] J. Gaubicher, C. Wurm, and G. Goward, "Rhombohedral Form of $Li_3V_2(PO_4)_3$ as a Cathode in Li-Ion Batteries," *Chemistry of Materials*, vol. 2, no. 23, pp. 3240–3242, 2000.
[36] P. P. Kumar and S. Yashonath, "Ionic Conduction in the Solid State," *Journal of Chemical Science*, vol. 37, no. 24, pp. 135–154, 2006.
[37] K. Nagamine, K. Hirose, T. Honma, and T. Komatsu, "Lithium ion conductive glass-ceramics with $Li_3Fe_2(PO_4)_3$ and YAG laser-induced local crystallization in lithium iron phosphate glasses," *Solid State Ionics*, vol. 179, no. 13–14, pp. 508–515, 2008.
[38] B. V. R. Chowdari, G. V. Subba Rao, and G. Y. H. Lee, "XPS and ionic conductivity studies on Li_2O-Al_2O_3-(TiO_2 or GeO_2)-P_2O_5 glass-ceramics," *Solid State Ionics*, vol. 136–137, pp. 1067–1075, 2000.
[39] J. Fu, "Fast Li^+ ion conducting glass-ceramics in the system Li_2O–Al_2O_3–GeO_2–P_2O_5," *Solid State Ionics*, vol. 104, no. 3–4, pp. 191–194, 1997.
[40] B. Smith, "Fundamentals of Fourier transform infrared spectroscopy," in *(CRC Press/Taylor and Francis, Boca Raton, FL)*, 2011, pp. 1–198.
[41] H. N. Majid, "Scanning Electron Microscopy," *BAOJ Microbiology*, vol. 1, no. 1, pp. 1–8, 2015.
[42] M. Dunlap and J. E. Adaskaveg, *Introduction to the Scanning Electron Microscope: Theory, Practice & Procedure*. FACILITY FOR ADVANCED INSTRUMENTATION, 1997.
[43] X. Xu, Z. Wen, J. Wu, and X. Yang, "Preparation and electrical properties of NASICON-type structured $Li_{1.4}Al_{0.4}Ti_{1.6}(PO_4)_3$ glass-ceramics by the citric acid-assisted sol-gel method," *Solid State Ionics*, vol. 178, no. 1–2, pp. 29–34, 2007.
[44] R. Alias, "Structural and Dielectric Properties of Glass – Ceramic Substrate with Varied Sintering Temperatures," *Materials Science: Sintering applications*, pp. 90–118, 2013.